

The Pennsylvania State University
The Graduate School
Department of Electrical Engineering

**AN AUTOMATED FIBER POSITIONING MECHANISM
FOR LIDAR APPLICATION**

A thesis in
Electrical Engineering

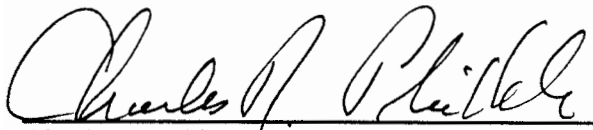
by
Anita S. Venkatarao

Submitted in Partial Fulfillment
of the Requirements
for the degree of

Master of Science
August 1994

We approve the thesis of Anita S. Venkatarao.

Date of Signature



Charles R. Philbrick
Professor of Electrical Engineering
Thesis Advisor

23 June 1994



Iam-Choon Khoo
Professor of Electrical Engineering

6/16/94

Larry C. Burton
Professor of Electrical Engineering
Head of the Department of Electrical Engineering

Abstract

An automatic beam alignment mechanism for a monostatic lidar system has been designed and tested. The raw lidar data consists of photon count of the laser return, which are detected after scattering by molecules and particles in the target volume. The signal received by the telescope is channelled to the detector by the optical fiber. Since maximum detected signal is desired, it is crucial therefore to feed all the collected light into the aperture of this optical fiber. In practice however, it was frequently observed that after the laser beam of the LAMP instrument was perfectly aligned in the field-of-view of the telescope, at a later time was found to have moved by a significant fraction of the beam spot diameter in the transverse plane with respect to the optic axis of the fiber. A direct way of sensing this motion and correcting it has been realized by using a quadrant detector as a sensor. The error in beam alignment is quantified by differential quadrant currents, which are converted to voltages and are used to set a timer, that controls the drive of a DC motor. DC motors, are mounted on the x and y-axes of the translation stage, providing the necessary movement to reposition the detector, and hence the fiber, relative to the beam. This active closed loop control system completes one cycle in about 10 seconds.

Table of Contents

	Abstract..	i
	Table of Contents	ii
	List of Figures	iv
	List of Tables	v
	Acknowledgements	vi
Chapter 1	Introduction.	1
	1.1 The LAMP Lidar Instrument	2
	1.2 Optical Alignment in Lidar Systems	3
	1.3 Layout of the Thesis	6
Chapter 2	Alignment.	7
	2.1 Approach to Automatic Alignment	7
	2.2 Types of Automatic Alignment	8
	2.2.1 Signal Maximization Method	9
	2.2.2 CCD Camera	10
	2.2.3 The Quadrant Detector	10
Chapter 3	Design of the Beam Alignment Mechanism	12
	3.1 Design of the System.	12
	3.1.1 Error Detection Module	12
	3.1.2 Error Correction Module	14
	3.2 The Quadrant Detector.	15
	3.3 The Electrometer Circuit	15
	3.4 The Control Circuit	19
	3.4.1 Circuit Description	20
	3.4.2 Design Calculations	22
Chapter 4	Tests and Analysis	24
	4.1 Defining the Problem of Alignment	24
	4.1.1 Quantifying Beam Alignment	24
	4.1.2 Verification of the Response from the Detector.	25
	4.1.3 Detector Response in the LAMP System	27
	4.2 Test Fixture Development	31
	4.2.1 The Electrometer Circuit	31

4.2.2	The Control Circuit	34
Chapter 5	Conclusions	38
	References	40
Appendix A	The Quadrant Detector (Silicon Detector Corporation)	41
Appendix B	The Electrometer Circuit	43
Appendix C	The Control Circuit.	45

List of Figures

1.	A schematic representation of the LAMP lidar system	4
2.	Design of the Automatic Beam Alignment Mechanism for the LAMP System	13
3.	Image points of near and far field objects	16
4.	The electrometer circuit used with the quadrant detector	17
5.	Modes of operation of the AD2101	18
6.	Control system design for single axis translation	21
7.	Lidar signal detected by the PMT as the fiber is scanned past the focal point.	26
8a.	Movement of the laser beam spot on the quadrant detector surface	28
8b.	Response of the quadrant detector to movement of the beam spot.	29
9.	Currents in quad cells 'A' and 'D' when the detector was installed in the LAMP system	30
10.	Test setup of the electrometer circuit	32
11.	Response of the electrometer circuit	35
12.	Test setup of the control circuit	36

List of Tables

1. Logic of the control circuit37

Acknowledgements

I would like to thank my advisor, Dr. C. R. Philbrick for guiding me through a rewarding research experience. I would also like to thank Dr. I.C. Khoo, for helping me and being on my committee.

Valuable help and advise given to me by S. Rajan, R. Smith, T. Kane, L. Marshall, M. O'Brian, S. Damodaran, D. Machuga, B. Mathason, S. McKinley, G. Pancost, L. Kellerman, and J. Corl, is gratefully appreciated.

Thanks are due to the Applied Research Laboratory, and the Communications and Space Sciences Laboratory, for providing their support in completing my work successfully.

It would be unworthy of me if I did not acknowledge the support and help offered by my husband. I would not have gone far without him. My 4-month old daughter, Sumana, deserves a special mention for giving me abundant time to work. I would also like to thank my in-laws for taking care of Sumana during my work.

Chapter 1

Introduction

Studies of the Earth's atmosphere have surpassed the realm of academia and become an element of interest to the common man, due to the growing concerns surrounding it. Remote atmospheric sensing techniques are favored over in situ measurements as they allow measurements on a larger scale. Traditionally, remote sensing relied on the blackbody emission of radiation and solar backscatter from atmospheric species. The invention of radars was a giant step forward in remote sensing technology. Radar (Radio Detection And Ranging) transmits radiowaves into the atmosphere, and analyses the backscattered return for various atmospheric characteristics. Lidar, also known as a 'Laser Radar', uses electromagnetic waves in the optical range as the active signal. Lidar has become popular during the recent past, because, it has higher angular resolution and better accuracy than a conventional radar for target tracking. Atmospheric molecules have a larger backscattering cross-section at optical wavelengths, which makes lidar a better technique for remote sensing. Many comprehensive articles on the techniques used in laser monitoring of the atmosphere are available [1,2,3].

Lidar is an acronym for Light Detection And Ranging. Lidar systems use various optical scattering processes from the atmospheric species to obtain spatially resolved measurements in real time. Lidars can also measure the quantitative attributes of the target region. A more detailed discussion on the scattering processes can be found in several references [4,5]. Laser backscatter from atmospheric scatterers is dependent on numerous

factors, such as, the shape and size of the particle, the index of refraction of the particle and the frequency of the incident laser. Specific properties of the target region may be assessed by suitably tuning the incident laser or selecting particular range of received frequencies. This ability of lidar techniques to perform effective spectral analysis of a distant target, has added a new dimension to remote sensing and opened a diverse range of applications. The LAMP (Lidar Atmospheric Measurements Program) lidar instrument at Penn State University provides profiles of temperature and density of the troposphere, trace constituents such as water vapor, as well as aerosol and cloud extinction and other atmospheric parameters. A brief review on the LAMP system is given in Section 1.1. More detailed discussions on the system can be found in several reports [6,7,8].

1.1 The LAMP Lidar Instrument

The LAMP instrument uses transmitting wavelengths of 532 nm and an ultraviolet wavelength, either 355 nm or 266 nm, to determine the various atmospheric conditions. The LAMP instrument consists of five principal subsystems: transmitter, receiver, detector, data system and the safety system. The Nd:YAG laser is used to transmit 20 pulses per second of 1.5 joules per pulse at 1064 nm. The fundamental frequency is doubled and tripled by nonlinear crystals to produce outputs at wavelengths of 532 and 355 nm. The final energy output is about 500 mJ at 532 nm and 200 mJ at 355 nm. The laser energy is directed out into the atmosphere with a beam expander and three laser hard-coated mirrors. The receiver is a f/15 Cassegrain telescope with a focal length of 6.09 m. Eight independent photomultiplier tubes (PMTs) are employed as detectors for different

wavelengths and altitude ranges. The output received at each channel is either digitized, or photon counted depending on the intensity of the signal and the dynamic range needed for that measurement. The signals are integrated by CAMAC data acquisition modules. The contents of the data register in the CAMAC crate are transferred once a minute, to the 486 PC where it is stored on an optical disk. The safety devices include laser interlocks, control panel panic buttons and an aircraft detection radar system.

The operation of the LAMP system is indicated in Figure 1. The backscattered light received at the telescope is collimated and channelled through an optical fiber cable. The amount of light or rather the photon count of the respective channels provides a measure of the atmospheric properties such as density of water vapor, aerosol profiles, etc.

1.2 Optical Alignment in Lidar Systems

Information about the atmospheric properties from lidar data is obtained by analyzing the laser backscatter received by a telescope. In earlier lidar systems the receiver optics and detectors and preamplifier electronics were attached to the back of the telescope. The signal was transferred from the focal plane of the telescope to the detectors by beam forming optics. The actual detectors were photomultiplier tubes which had high sensitivity, low noise, and a good quantum efficiency over a sufficiently wide spectral range. Silicon photodiodes and charge coupled devices (CCD) have also been used in the

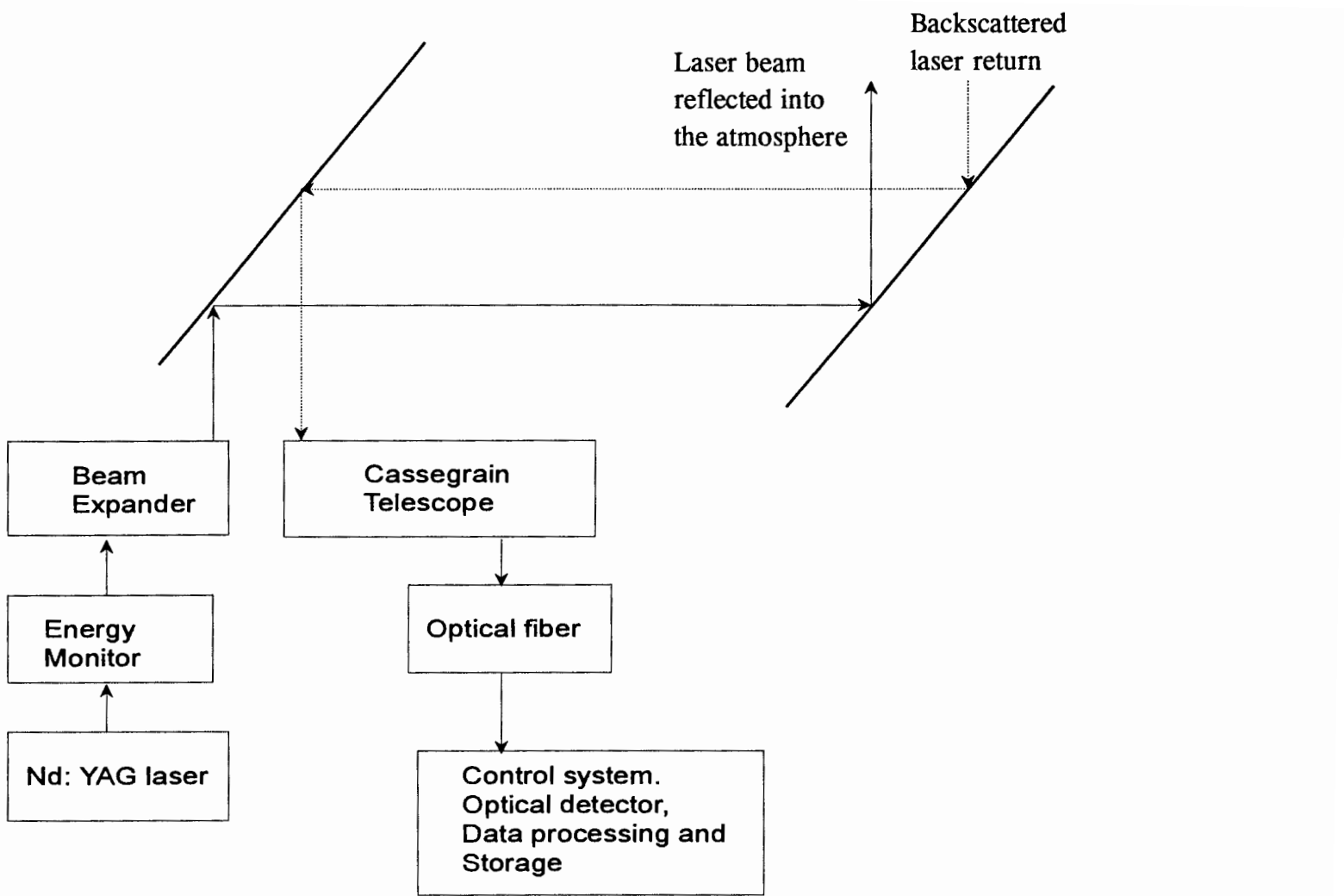


Figure 1. A schematic representation of the LAMP lidar system.

area of photometric instrumentation [9] with the advantage that, in the infrared region, silicon detectors have a higher quantum efficiency than photomultiplier detectors. However, lidar systems have been used more extensively in multi-element spectroscopy where multiple channels are needed to process data from the same return. These additional detectors made it more difficult to attach them behind the telescope. The use of optical fibers in lidar systems made it possible to isolate the detector electronics from the telescope to minimize ground loops and electromagnetic interference. With optical fibers it is possible to achieve a high degree of electrical isolation and noise immunity. The fiber optic cable would act as an optical transmission line to couple the focal plane of the telescope to remote detectors allowing flexibility in the layout of the instrument. While the telescope receiver may be located for efficient data collection, the detector and electronics may be kept in a dust-free and controlled environment.

Though it may seem straightforward to use optical fibers to couple a signal from the focal plane of the telescope to isolated detectors, many factors influence the photometric precision of these measurements. Optical transmission through a fiber can be reduced by many factors, some of which include: changes in the position of the image with respect to the center of the fiber, dust on the fiber end-faces, movement of the coupling optics, and changes in the bend radius of the fiber. The problem addressed here is the monitor and control of the image spot in the receiving plane of the fiber. A likely way of automating the detection and correction of the problem is the theme of this thesis.

One way to limit the problem of aligning the image spot with the center of the fiber is by widening the field-of-view (FOV) of the telescope. This minimizes the beam spot

diameter and hence reduces the sensitivity of the system to small alignment errors. This is however, not a practical solution, because, increasing the field-of-view involves using a fiber of a larger diameter, or altering the focal length of the telescope. Moreover in a system designed to obtain quantitative measurements of the atmosphere, it is essential to minimize errors in instrumentation as much as possible.

In the LAMP system the image spot wanders on the fiber surface for several reasons. Correcting for each one of those factors is not only tedious, but an effective solution is hard to verify. An automatic mechanism for detecting and correcting any changes in the beam alignment in the receiving plane of the fiber is necessary. An active method of detecting this drift has been developed which uses a quadrant detector as its primary sensor. The development and testing of this advancement is the central idea of this thesis.

1.3 Layout of the Thesis

An automatic method of detecting and correcting any variations in aligning the laser beam with the center of the optical fiber has been developed and tested in this research effort. Chapter 2 poses alignment problems and reviews the available solutions leading to the rationale behind the use of the quadrant detector. Chapter 3 details the design of the system. The various tests conducted and an analysis of the results obtained are described in Chapter 4. In Chapter 5 the conclusions are followed by a discussion of future work.

Chapter 2

Alignment

The laser backscatter radiation received by the telescope must be centered on aperture of the optical fiber. Also, the angle of rays from the telescope must lie within the numerical aperture of the optical fiber. If the light falls outside the fiber surface, it remains undetected by the PMT and hence results in a loss of signal. This reduced signal at the PMT has two important consequences. First, it results in a loss of signal identified by the telescope. Second, it results in a nonlinear relation between the incident laser and the backscattered return detected at the telescope.

2.1 Approach to Automated Alignment

In the LAMP system the image spot moves on the fiber for several reasons. As with most mechanical instruments, no matter how robust their construction, the lidar is susceptible to thermal changes, which degrades its performance. The beam instability of the transmitter could result in spurious changes in beam spot diameter. The beam pointing stability of the Continuum NY81-20 laser is about $250\mu\text{rads}$. The image spot can also move because of the mechanical flexing of the system when the telescope is moved in and out of the trailer, or even when an operator moves about in the trailer.

In the LAMP system, whenever the beam drifts from the field of view of the fiber, several techniques have been suggested to correct for the misalignment. One approach is to change the position of the mirror by using computer control so that the beam is

redirected completely into the fiber. This technique was effective but proved to be tedious and cumbersome since the source of the problem and the point of actuation were located away from each other. Also the test was conducted only between data taking intervals. This method of realignment was tested by manually operating the micrometer screw in the mirror or the translation stage mount for the optical fiber. The "aligned" position is identified by the operator. This scheme could be improved by practice, but is limited by the resolution of human eye and manual dexterity. The procedure can be automated by using computer control which would require additional effort in writing new software. An automatic means of continuously detecting and correcting for beam misalignment has become essential for the LAMP instrument.

2.2 Types of Automatic Alignment

Several types of automated beam alignment have been considered since the problem surfaced. These include :

- a. signal maximization method,
- b. use of the CCD camera, and
- c. use of the quadrant detector.

The advantages and disadvantages of each one of those techniques are described below. The CCD camera and the quadrant detector have been examined in some detail with reference to the LAMP system, and the signal maximization method is normally used in aligning the instrument.

2.2.1 Signal Maximization Method

The optical fiber is essentially an optical transmission line that transmits light incident on one of its end-face to the other. The amount of light transmitted is maximum when the beam is centered with respect to the fiber and the ray path angle is within the numerical aperture of the fiber. One way to detect any variations in the position of the incident beam on the fiber end-face would be from the reduction in signal. Correction is accomplished by moving the fiber position until a maximum signal, indicating the amount of light into the fiber, by using a control algorithm. The amount of light detected by the PMTs in a chosen range bin could be used as the input parameter. The algorithm would use the signal received from the range bin and direct a stepper motor optimally to maximize that signal level.

Positioning the fiber for maximum signal level is a very sensitive method since the program can be customized to individual systems. Small variations in the program would extend its utility for other altitudes and different atmospheric conditions. This method is limited by reduced signal levels at the PMT due to fluctuations in the incident laser beam, changing atmospheric conditions during the test, or variations in the detected signal. In order to eliminate the other factors and narrow down the prospective cause for signal reduction to beam misalignment, the algorithm may require some time to converge. Moreover the test is also limited to times between data runs.

2.2.2 CCD Camera

The second method considered uses a charge coupled device (CCD) camera whose photosensitive surface area is divided into a pixel grid. A small fraction of the laser return at the telescope is directed toward the CCD surface. The pixels are illuminated by the incident beam. By virtue of its near Gaussian distribution of energy, the laser beam is the brightest at the center. The CCD can be programmed to seek the pixel of maximum intensity and the optical fiber aligned accordingly. This is one of the more popular techniques used in astronomy in locking on stars and satellites.

This technique is limited for applications to the lidar system because of the reduced contrast that is obtained during daylight. Moreover, the beam tends to misalign quite frequently. This would require the CCD camera to memorize the "aligned" position and react faithfully every time the beam drifts from this position. The aligned position is a statistical average of the spot during a scan period. One concern is that the CCD exhibits hysteresis. This property identifies the error differently when operated in the forward and reverse modes. In using the error signal identified by the CCD for alignment purposes, this property renders it deficient for two way actuation.

2.2.3 The Quadrant Detector

A quadrant detector is proposed as an alignment aid. The photosensitive surface of this detector is divided into four quadrants, each quadrant separated from the other by a gap. The detector has a hole in the center that can be used as a window for the optical fiber. The end-face of the optical fiber is held flush with the photosensitive surface of the

detector. When the beam is absolutely centered with respect to the fiber-detector assembly, the currents in the four photoconductive quadrants are nearly equal. When the beam wanders from this "aligned" position, one of the quadrants collects more of the signal and is illuminated more than the others. This increases the current produced by that quadrant relative to the currents in other quadrants and identifies the change in the position of the beam. Appropriate corrective measures are taken to move the fiber-detector assembly so that the light is recentered into the fiber, and the currents in the quadrants of the detector are equal.

This is a novel technique since misalignment is detected directly by the sensor and is not inferred from related parameters. Simple and repeatable photoconductive properties of the detector are employed directly to make the correction. The test can be used during data runs. These factors set this mechanism apart from the others.

The quadrant detector has several significant advantages over the use of a CCD camera. First, in using a CCD camera for alignment purposes, a part of the return collected at the telescope is directed toward the CCD camera. The quadrant detector proves to be a more efficient tool, since it collects any light that spills outside of the fiber. Second, the aligned position identified by the CCD is a statistical average of the image spot. The quadrant detector, on the other hand, provides an active and continuous means of alignment. Additionally, the quadrant detector is less expensive than the CCD camera.

Chapter 3

Design of the Beam Alignment Mechanism

The automatic beam alignment mechanism, which uses the quadrant detector, is controlled in a closed loop system. An off-center beam creates an error signal at the quadrant detector. The control circuit operates on this error signal and moves the detector-fiber assembly until the error signal is minimized. For descriptive purposes, the design elements of the system are divided into two modules. The design of the system is stated briefly in the next section. The electrical circuit and supporting calculations are described in a later part of this chapter.

3.1 Design of the System

The block diagram of the unit operation is shown in Figure 2. The designed system could be represented by two basic functional modules, the error detection module and the error correction module.

3.1.1 Error Detection Module

The laser light that is scattered from various particles in the atmosphere is collected by the telescope, collimated, and directed into the optical fiber. The optical fiber is located at the effective focal plane of the telescope. The receptive end of the optical fiber is held flush with the photosensitive surface of the quadrant detector and in the center bore. Light from far field should lie within a 0.2 mm blur circle for the Cassegrain telescope.

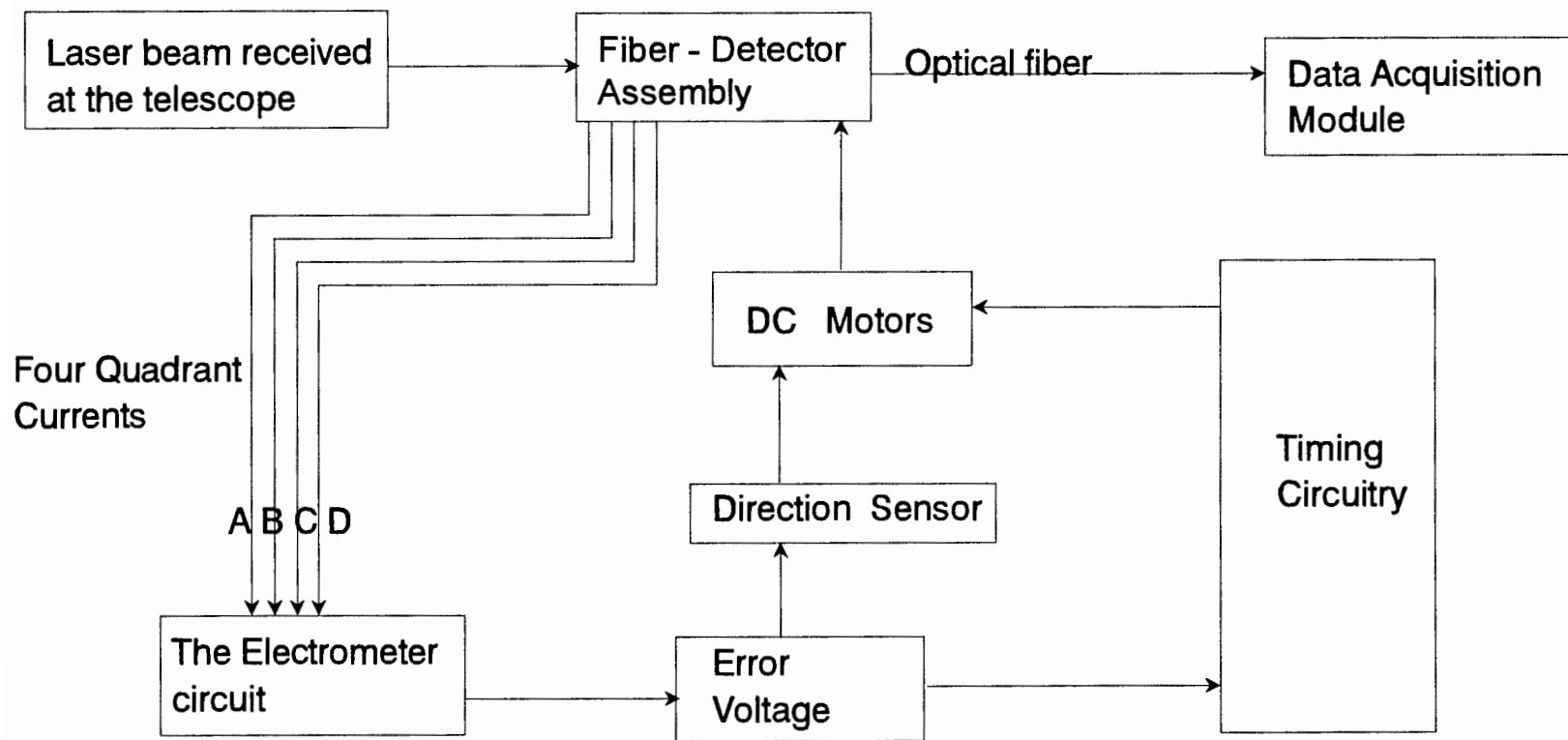


Figure 2. Design of the Automatic Beam Alignment mechanism for the LAMP system

In the near field, within the range of 1 km, the blur circle increases and eventually overfills the 1 mm fiber. When the beam moves from the center of the field-of-view, it illuminates one or more of the four quadrants of the detector. The photoconductive surface of the detector emits currents, that are integrated and converted to voltages. An electrometer device, used to convert current to a voltage, was designed and used as the 'error detection module'. The mathematical difference of the voltages from two opposing quadrants represents the error in alignment. Two error voltages represent displacement along the two axes in the transverse plane of the beam.

3.1.2 Error Correction Module

To correct for the shift in beam position off-center from the optical axis, the translation stage that houses the quadrant detector and the optical fiber is moved. Two DC motors are used, one for each of the axes that represent the orthogonal plane of the beam. Control of either motor is provided by timing the interval during which power is supplied to the DC motors, and hence moving the stage in short steps of a selected interval. The magnitude of error voltage determines how long the motors must be propelled to obtain the required translation. The direction of linear actuation depends on the polarity of the error voltage. In defining the transfer function that relates the error voltage to the necessary time interval, extensive calculations were done which will be discussed in Section 3.4.2.

3.2 The Quadrant Detector

The quadrant detector which is used as a primary position sensor is the SD225-23-21-040, manufactured by Silicon Detector Corporation. Its details are outlined in Appendix A. This component is somewhat unique, in the sense that it is made with a central hole slightly greater than 1 mm. This suits our purpose in the LAMP system, since the optical fiber used has a core diameter of 1 mm, and an outer diameter of 1.8 mm. The detector has four photosensitive quadrants and a hole in the center 1.27 mm in diameter. When the protective cover of the fiber is partly stripped back, its cladding diameter makes a close fit into the central bore of the quadrant detector.

3.3 The Electrometer Circuit

The electrometer circuit has been designed to produce a DC voltage proportional to the current in each photodetector quadrant. A basic integrator is used to convert the current from each quad cell in the detector to a voltage. The laser pulses that are fired into the atmosphere are 8 ns wide, while successive pulses are 50 ms apart. If the integrator accumulates continuously, it would average the laser pulse return energy over the entire 50 ms period, which would result in a small value. It is therefore necessary to gate the integrator such that it can integrate for only a part of the entire cycle. In order to collect light from say, 'x' km, the integrator has to be gated for a minimum of $2 * x/c$ seconds, to allow for two-way travel time (c is the speed of light). It is chosen to integrate all of the return light from the surface to 2 km altitude for alignment purposes. This is because the return signals from each scattering volume, at successive altitudes, are focussed at

different points along the optical axis of the telescope. When the fiber is located at the prime focus (effective focal point) of the telescope, light from the far field is imaged into a spot diameter of 0.2 mm and is directed completely into the fiber. Light from lower altitudes focusses behind the aperture of the fiber. However, this light from lower altitudes illuminates the detector around the fiber, and is used for alignment purposes. Figure 3 explains this concept. To collect returns up to 2 km the integration time has to be a minimum of $13.3 \mu\text{s}$. The designed integrator collects current for $20 \mu\text{s}$ after the

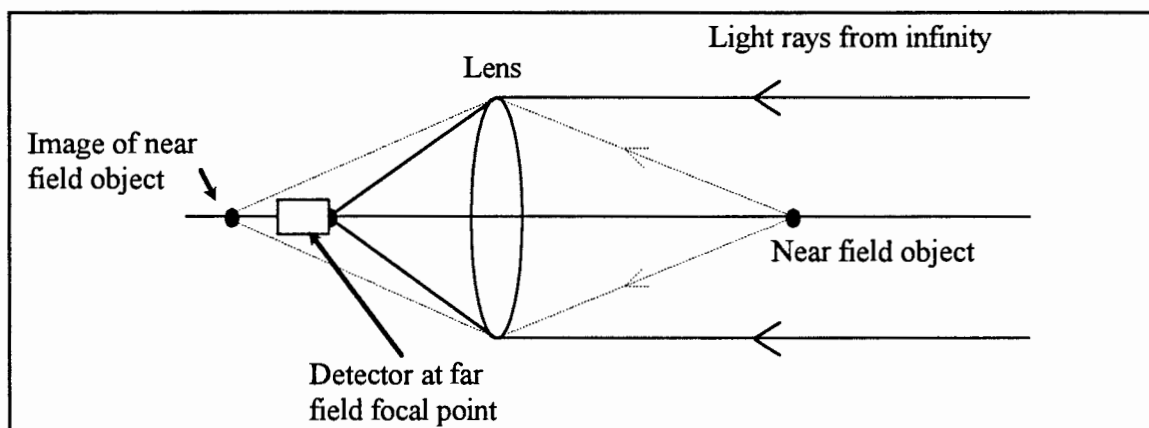


Figure 3. Image points of near and far field objects

rising edge of the laser pulse. The circuit which has been prepared is shown as a block diagram in Figure 4. The actual circuit is presented in Appendix B. The range of currents expected from the quadrant detector is in the order of a few 10's to 100's of nA. Hence, a very sensitive integrator chip, AD2101, manufactured by Burr-Brown was used. The rest of the elements in Figure 4 form the timing circuit necessary for the working of the AD2101. The timing diagram shown in Figure 5 is useful in summarizing the characteristics of AD2101.

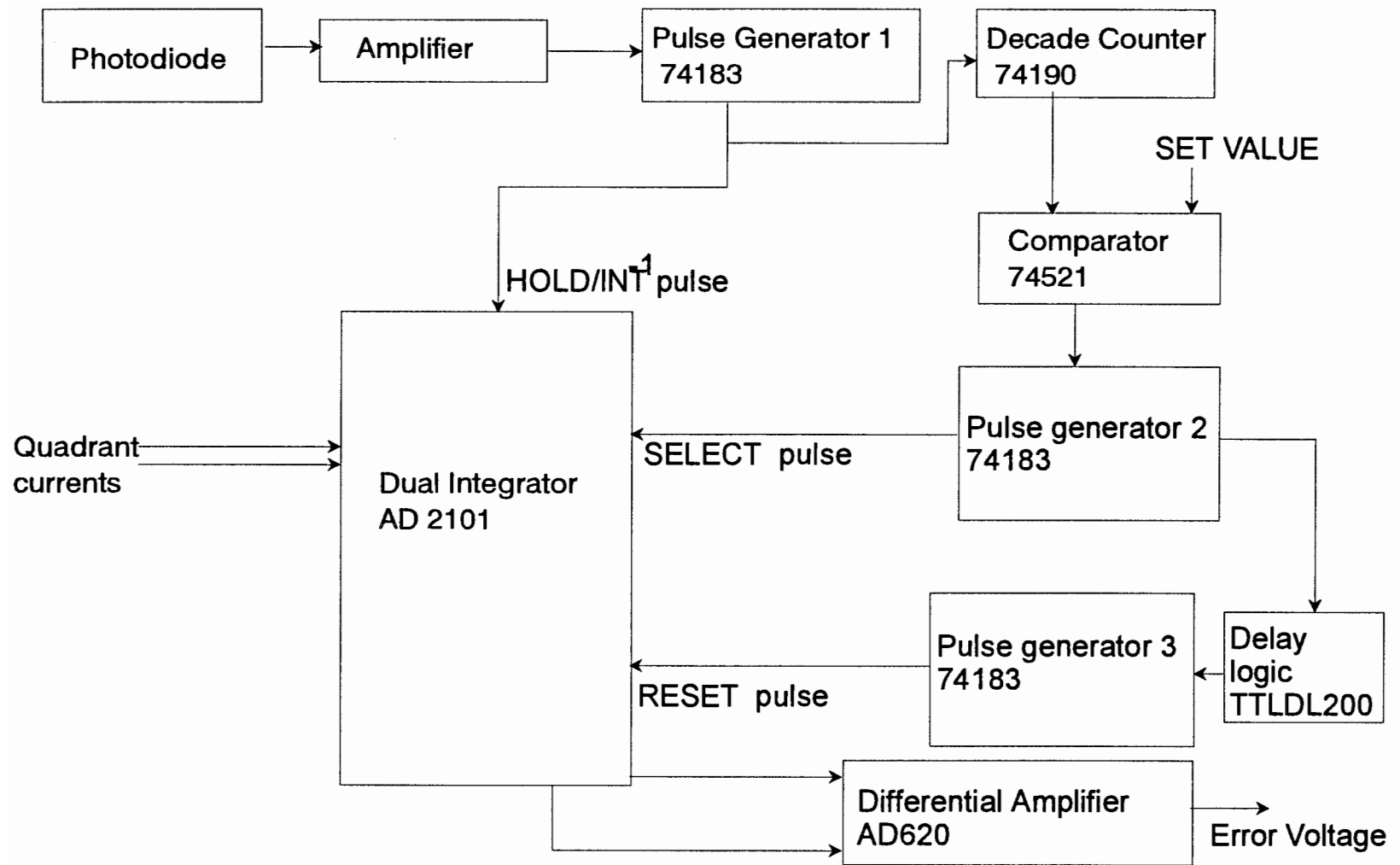


Figure 4. The electrometer circuit used with the quadrant detector

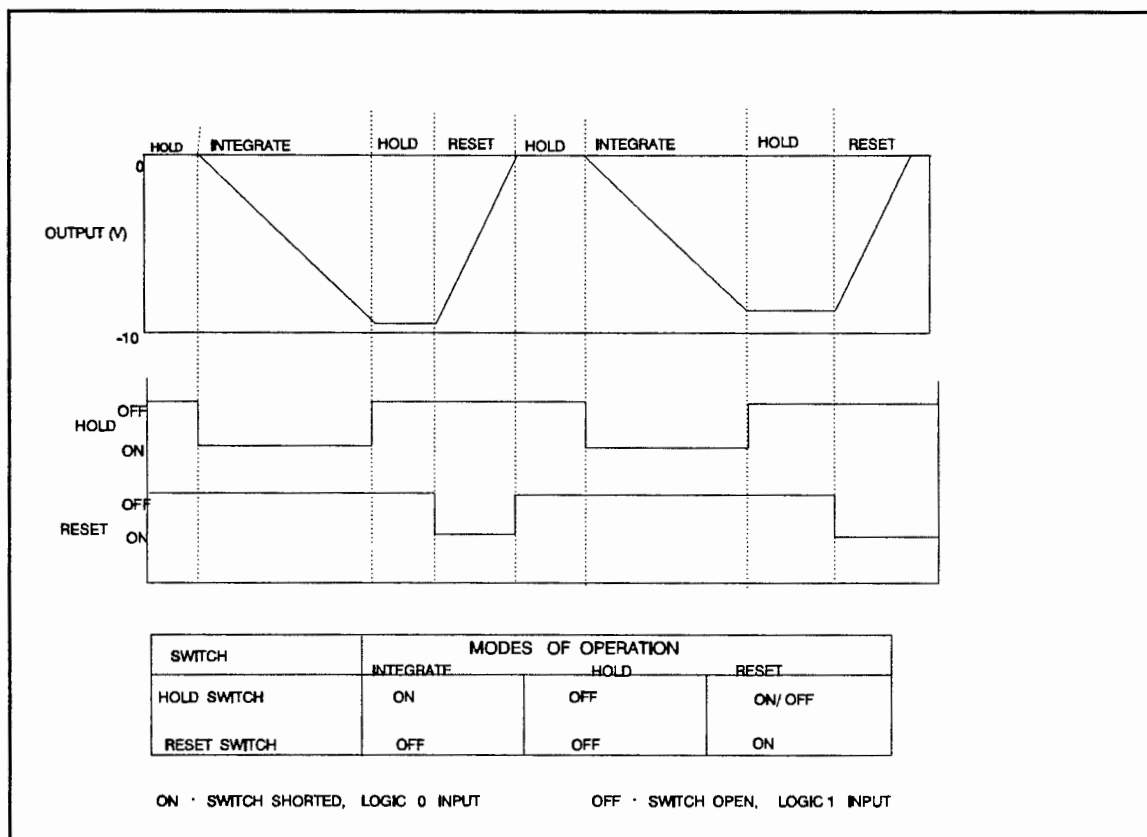


Figure 5. Modes of operation of the AD2101.

The AD2101 is a dual integrator that can be made to operate in one of the three modes, integrate, hold or reset. The device exists in one mode, or the other, depending on the logic levels of the three control signals; $HOLD/INT^{-1}$, $SELECT$ and $RESET$. The AD2101 can be made to integrate for a certain period or retain its most recent voltage level by keeping the $HOLD/INT^{-1}$ signal at a logic low or high, respectively, while maintaining the $RESET$ signal at a logic high level. To reset the device, the $RESET$ signal should be at a logic low, while the $HOLD/INT^{-1}$ is held high. The AD2101 is a dual integrator. One of the dual integrators may be chosen by forcing the $SELECT$ signal of that integrator

low, while maintaining the rest of the signals at a logic high.

A photodiode is placed in the laser container where it can sense the timing of every laser pulse fired into the atmosphere. This pulse from a laser shot generates a current pulse in the photodiode, which is used to enable a one shot generator. The 74183 generates a 20 μs pulse which is inverted to create the HOLD/INT⁻¹ signal for the AD2101. The error voltage is the differential voltage of two quadrants. It would not be worthwhile to compare the four quadrant voltages every laser shot, since the difference in two very small voltages would be smaller. Hence the comparisons are done after a preset number of pulses. The digital counter 74193 keeps track of the number of integrator gating pulses. Once the required number of pulses, typically 100 laser pulses, are counted, the comparator, 74521, generates a pulse that is used to enable another oneshot generator. The pulse from the last generator (74183), is used as the SELECT signal for the AD2101. All of the integrators are selected at the same instant, so that the error voltage is accurately represented. The circuit has to be reset before the next set of integrations occur. Toward this end, the SELECT pulse is used to gate a third one-shot generator. To ensure that the voltage is accurately read by the buffer, the SELECT and RESET pulses are separated by a time delay of 200 μs . The chip, TD200, is used to include the necessary delay. Both the SELECT and RESET pulses are 200 μs wide.

3.4 The Control Circuit

If the direction of beam propagation was considered to be along the z-axis then, the displacement of the image spot in the transverse plane of the fiber could be represented by

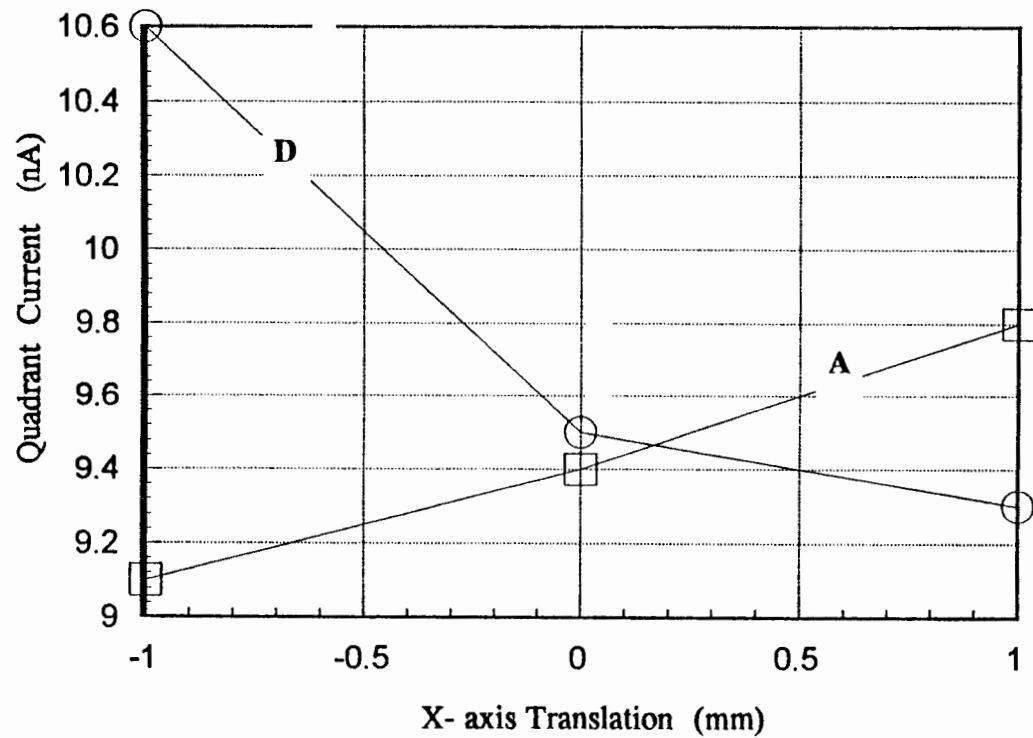


Figure 9. Currents in quad cells 'A' and 'D' when the detector was installed in the LAMP system.

movement in the x-y plane. Refer to the block diagram representation of the control circuit, Figure 6. The control circuit designed must be capable of moving the translation stage that houses the fiber-detector assembly along both axes for minimum displacement. Positive and negative movement along an axis is required for automation and control. Micrometers / DC motors have been used to provide translations along the two axes.

The control circuit uses the error voltage from the integrator comparator as the input control parameter. The absolute value of the error voltage determines the duration of actuation while the sign on the error voltage determines the direction of linear actuation.

3.4.1 Circuit Description

The linear actuation of the two axes of the translation stage is achieved by powering two motors. In the design, the motor is powered by current from a power transistor and the time interval for which the motors are on, determines how far the stage will travel. The absolute value of error voltage is used to determine the duration of the motor on time. The error voltage is continuously compared with the voltage on a capacitor that is being incremented linearly from a constant current source. The LM334, an analog chip manufactured by National Semiconductor, is a constant current source whose value is dependent, only on an external resistor. The LM314 compares the linearly changing voltage on the capacitor with the constant error voltage. The comparator switches "LOW" when the capacitor voltage exceeds the error voltage. The time duration required for the comparator to switch between the two logic levels, is a function of the error voltage. The transistor is biased by the current pulse from the comparator which determine the on-time

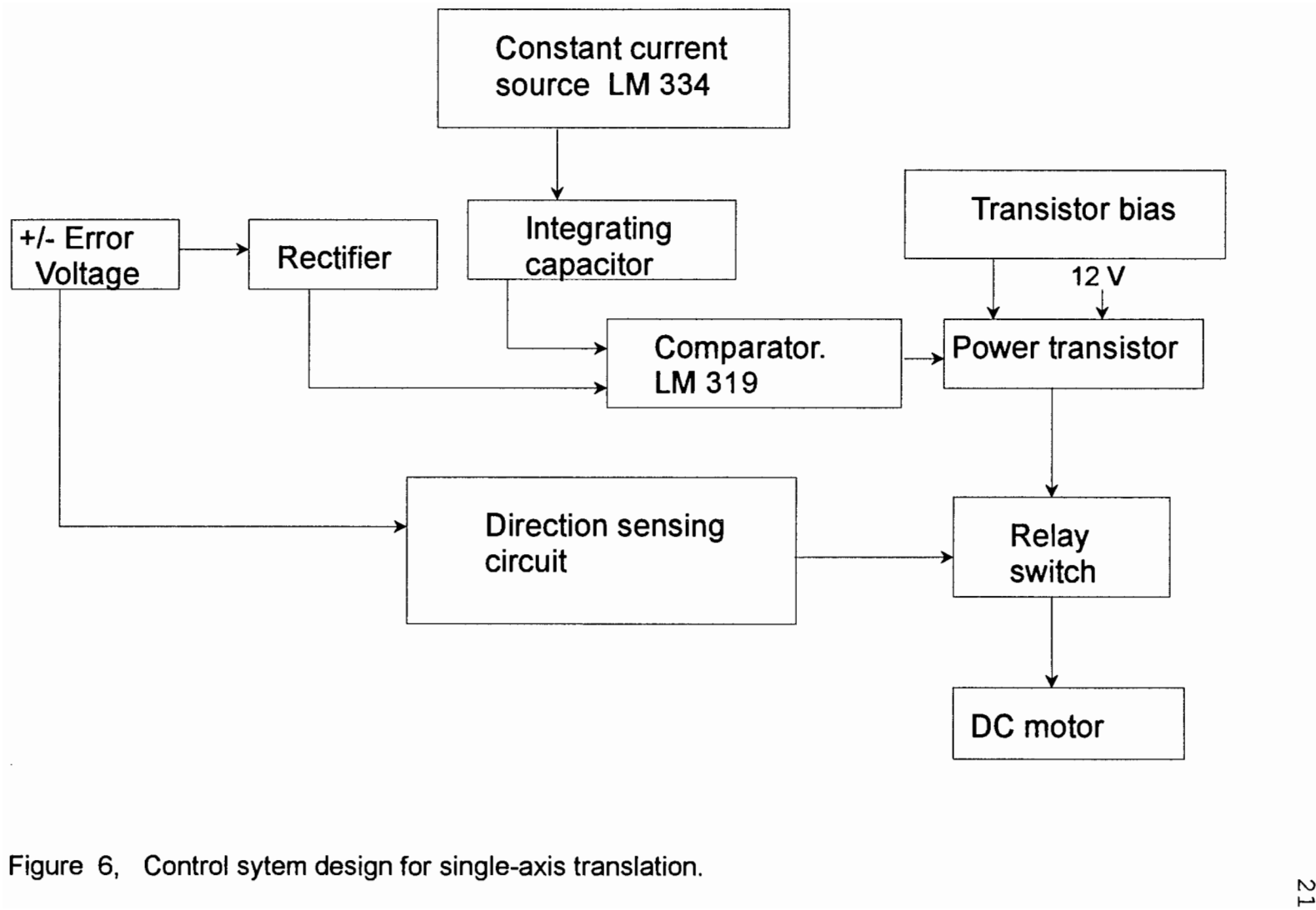


Figure 6, Control system design for single-axis translation.

of the motor.

The polarity of the error voltage determines the direction of linear actuation of the motor. A relay switch is used to reverse the connections on the motor and is activated to move the motor either way, depending on the sign of the error voltage. The calculations involved in the specific design of the control system for LAMP lidar are given in Section 3.4.2. The circuit schematic diagram is given in Appendix C.

3.4.2 Design Calculations

The speed of the DC motor, manufactured by NEWPORT (part number 860A-050) is 1467 rev/min/volt. With a gear deduction factor of 262:1 and a fixed voltage of 12 V, the speed of the motor becomes 1.12 rps. The linear motion of the motor is achieved by a lead screw whose pitch is 1/32". Hence the linear speed of the motor along the direction of actuation is 0.889 mm/sec. Basically the timing of the switching of the motor is decided by the rate at which the capacitor charges, which in turn depends on the value of the capacitor and current from the constant current source. The current from the constant current source, LM334, made by National Semiconductor, is a function of a resistor, R_{SET} ohms,

$$i \text{ (amperes)} = (63.7 \times 10^{-3}) / R_{SET}$$

The voltage V_C on capacitor C (Farads), due to the current from a constant current source is,

$$V_C \text{ (Volts)} = (i \times \Delta t) / C \text{ (Farads)},$$

$$\Delta t = \text{integrating time.}$$

Combining equations provides the relation,

$$V_C \text{ (Volts)} = (63.7 \times 10^{-3} \times \Delta t) / (R_{\text{SET}} \times C).$$

For particular values of R_{SET} and C , the error voltage determines the integrating time necessary for the capacitor to equal that voltage. During this time, the DC motors move a distance of

$$x \text{ (mm)} = 0.889 \times \Delta t.$$

In the aligned position, the beam diameter has to be a minimum of 1.5 mm. The outer diameter of the sensitive detector surface is 5.72 mm. This allows a maximum of +/- 2.11 mm travel distance by the motors. If the worst case of beam alignment is represented by an error voltage of 5V, then, the motor 'on' time is

$$\Delta t = 2.11 / 0.889 = 2.373 \text{ milliseconds.}$$

The design problem reduces to choosing values of R_{SET} and C , such that

$$R_{\text{SET}} \times C = 3.2 \text{ milliseconds.}$$

Chapter 4

Tests and Analysis

Various experiments were conducted to study the alignment and positioning of the beam. Initial tests were done to verify the capability of the quadrant detector for alignment control. A unit was constructed and tested at a breadboard level. The test setup was prepared exclusively to simulate alignment in the LAMP system as closely as possible. The results of these tests and the efficiency of the circuit are discussed at the end of this chapter.

4.1 Defining the Problem of Alignment

A beam that is off-center, with respect to the optical axis of the system, results in attenuation of the signal transmitted to the PMT. A quantitative analysis of this error in the LAMP system is presented. Quadrant detectors provide position information as a directly measured quantity with a high degree of precision and stability. Both the simulation of the response, and verification of the detector were done using the LAMP system.

4.1.1 Quantifying Beam Alignment

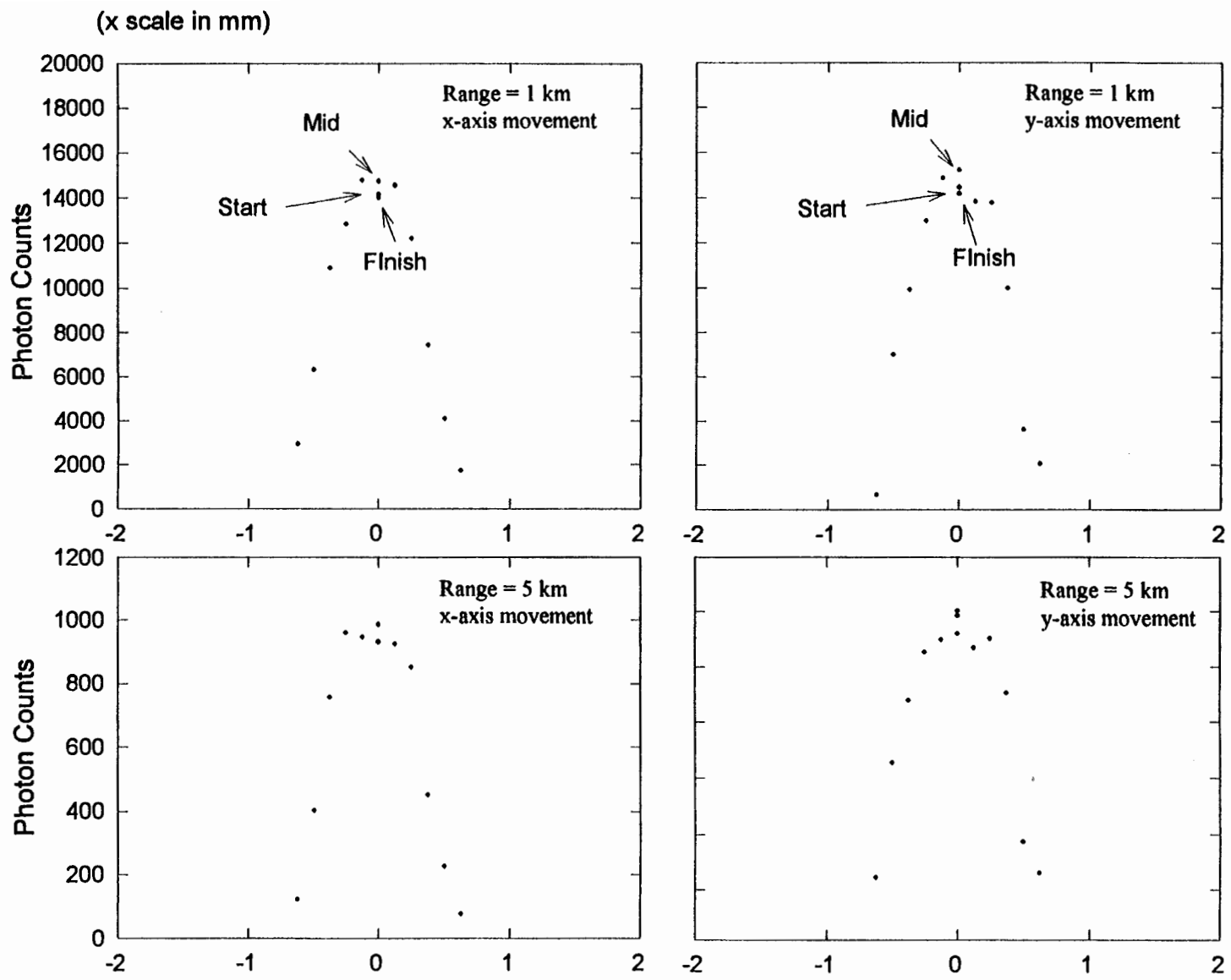
In the LAMP system the optical fiber is used as a transmission line to de-couple the detector from the receiver subsystem. If the beam path of the laser backscatter received by the telescope does not fall completely within the diameter of the fiber, then

all of the received light is not transmitted to the PMT. Additionally, the angles of light ray cone must be within the numerical aperture of the fiber. Figure 7 shows results of the photon count detected from a certain altitude when the optical fiber assembly is moved in the transverse plane of the beam. The changes in photon count from near and far field, specifically, returns from 1 km and 5 km altitude are compared. It was noted that when the beam moves from the fiber surface by 20% or more of the beam spot diameter, the photon count drops rather drastically. The falloff is less steep in the case of return from 5 km than 1 km, which implies that the signal received from 'far', field is focussed well into the fiber and hence less sensitive to beam misalignment than the return from 'near' field.

4.1.2 Verification of the Response from the Detector.

The photoconductive surface of the quadrant detector emits current proportional to the amount of light incident on it. If a beam that is radially symmetric about the optic axis is centered on the detector surface, the resulting currents from the four quadrants are nearly equal. The difference in sensitivity between the quadrants was measured by moving the beam fully onto each quadrant in sequence. The change in the position of the centered image spot relative to the quadrants of the detector, changes the currents proportionally. Experiments were conducted to verify that the behavior of all the quadrant currents corresponded to a proportional change in the position of the beam. The individual quadrant currents from the detector were recorded when the position of the laser beam spot of 1 mm diameter from the 1 mW continuous-wave (CW) HeNe laser was moved on the

Figure 7. Lidar signal detected by the PMT as the fiber is scanned past the focal point



surface of the detector. The quadrant detector, mounted on an XYZ translation stage, was placed in the path of the laser beam. The stage could be moved in the perpendicular plane of the beam by two micrometer screws. The position of the stage, when the currents from all the quadrants are equal, was identified. Initially the laser beam was incident completely on quadrant 'C' and then moved to quadrant 'D' in steps of 250 microns. The movement of the beam spot is indicated in Figure 8a. Figure 8b shows the responses of the four quadrant cells of the detector at every step change in the beam spot position.

As the beam spot position shifts from quad cell 'C' to 'D', the current produced by 'C' decreases and the current produced by 'D' increases. Though the beam was incident completely on quadrants 'C' and 'D' during the beginning and end of travel, the current produced in cells 'A' and 'B' also change, but the result is a smaller value of current.

4.1.3. Detector Response in the LAMP System.

The circuit had to be tailored to meet the requirements of the LAMP system. The laser backscatter received by the telescope creates a current in each quad cell of the detector, which is used as the primary input parameter in the closed loop circuit. It was necessary to identify the response of the detector when it was placed at the effective focal point of the telescope, which is the location of the optical fiber along the optic axis. The dark current of the quad cell, when the laser was turned 'off', was 6 nA. When the laser backscatter signal was centered on the detector, the current from each quad cell was about 9 nA. The position of the spot was changed by moving the mount relative to it and the

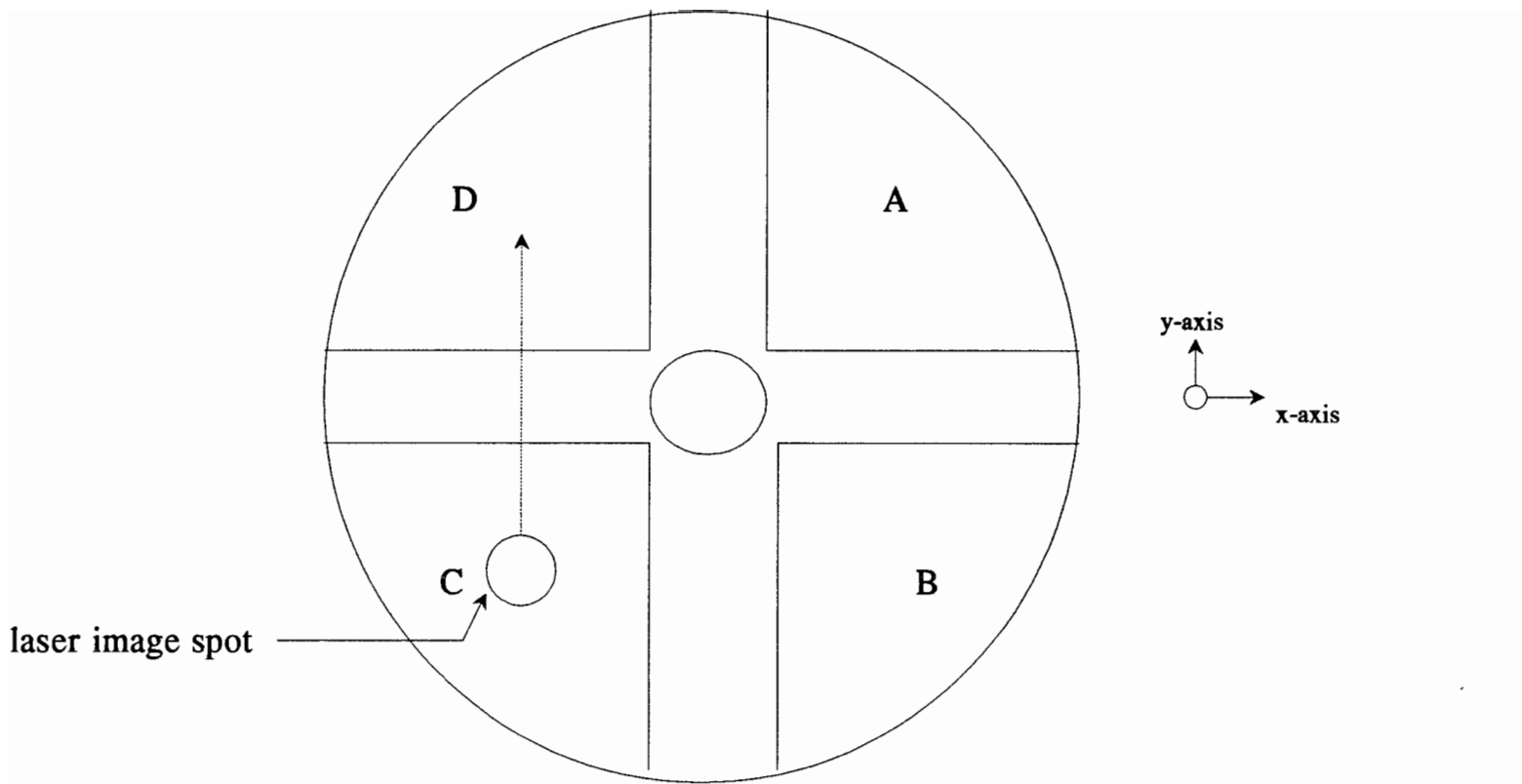


Figure 8a. Movement of the laser beam spot on the quadrant detector surface

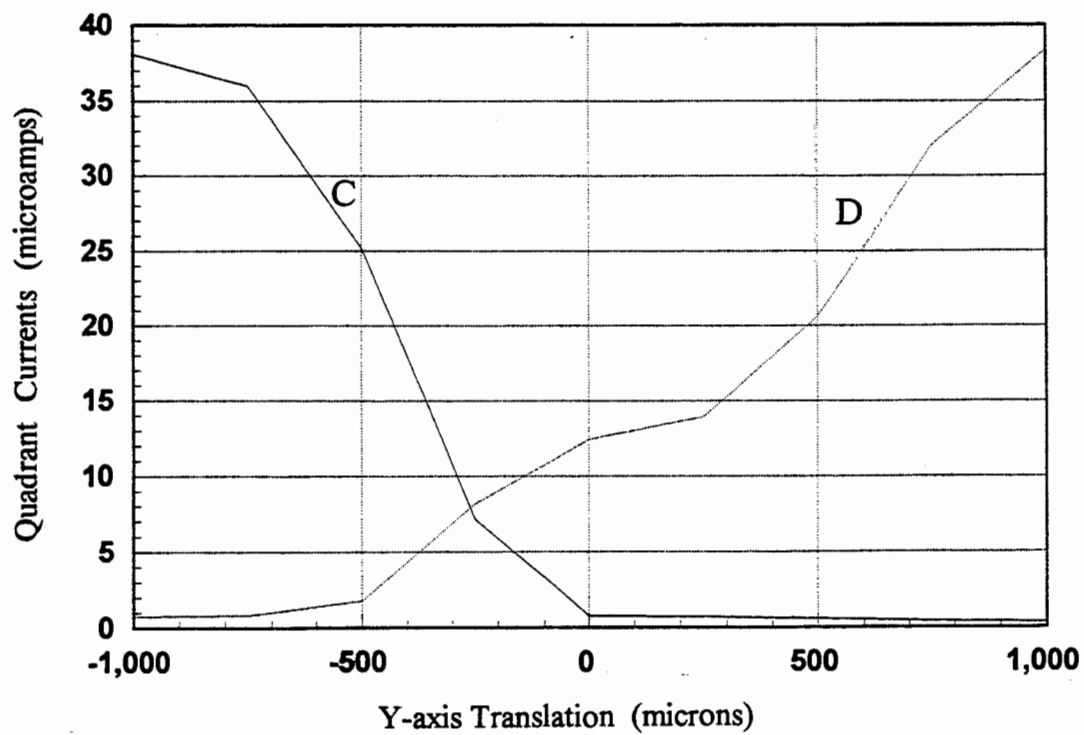
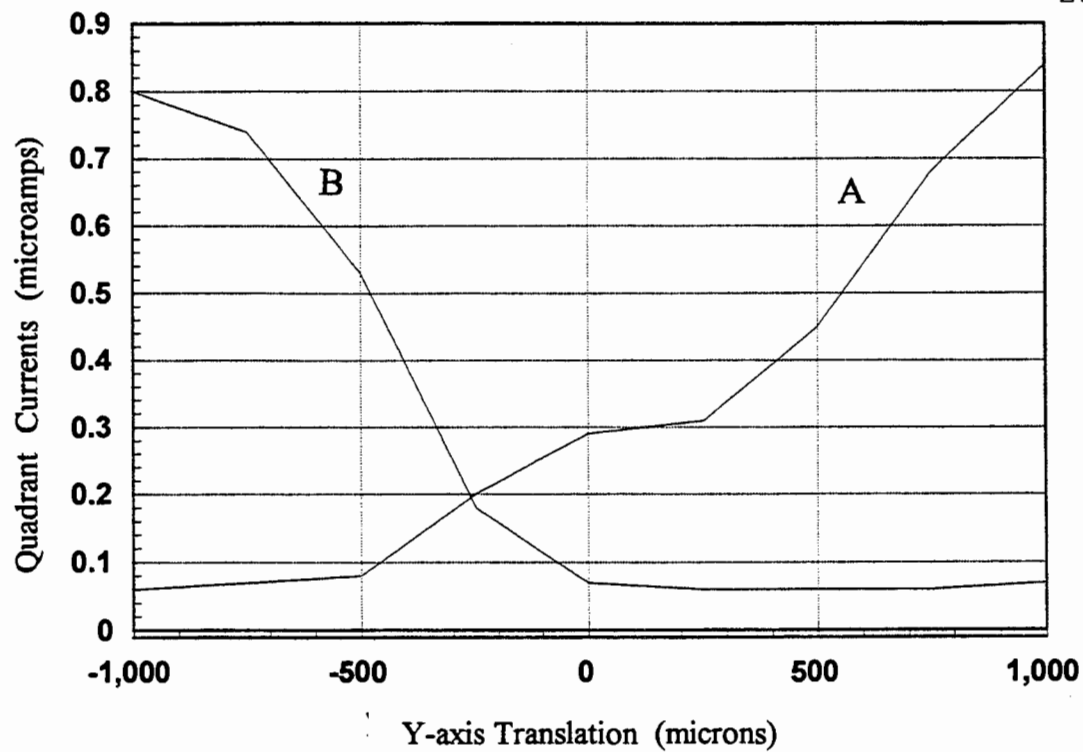


Figure 8b Response of the quadrant detector to movement of the image spot

change in currents in each quad cell was recorded. Figure 9 shows the currents in cells 'A' and 'D' when the beam spot was moved from cell D to cell A along the x-axis. The graph shows a decrease in the current produced by cell D and an increase in the current produced by cell A. Compared to the tests done with the CW HeNe source, the response of the detector in the LAMP system was lower, and also, the relative changes in response was not as large. This is because the meter used to measure the alternating current expects a square wave with a duty cycle of 50%. The Nd:YAG laser, however, fires laser pulses that are 8 ns wide and at a frequency of 20 pulses per second. The currents measured by the meter were an average over the entire 50 ms interval and hence of a lower value. In order to adapt the quadrant detector in the LAMP system, the signal identified by the telescope must be amplified greatly.

4.2 Test Fixture Development

The proposed beam alignment mechanism for the LAMP lidar was tested at a laboratory facility at Communications and Space Sciences Laboratory (CSSL) at Penn State University's Electrical Engineering Department. The electrometer and control circuits are described separately.

4.2.1 The Electrometer Circuit

The test setup, represented in Figure 10, shows the CW HeNe laser used as the incident light source. In order to obtain a pulsed laser output, the beam was intercepted by a chopper wheel. This wheel was completely dark, except for a narrow window cut

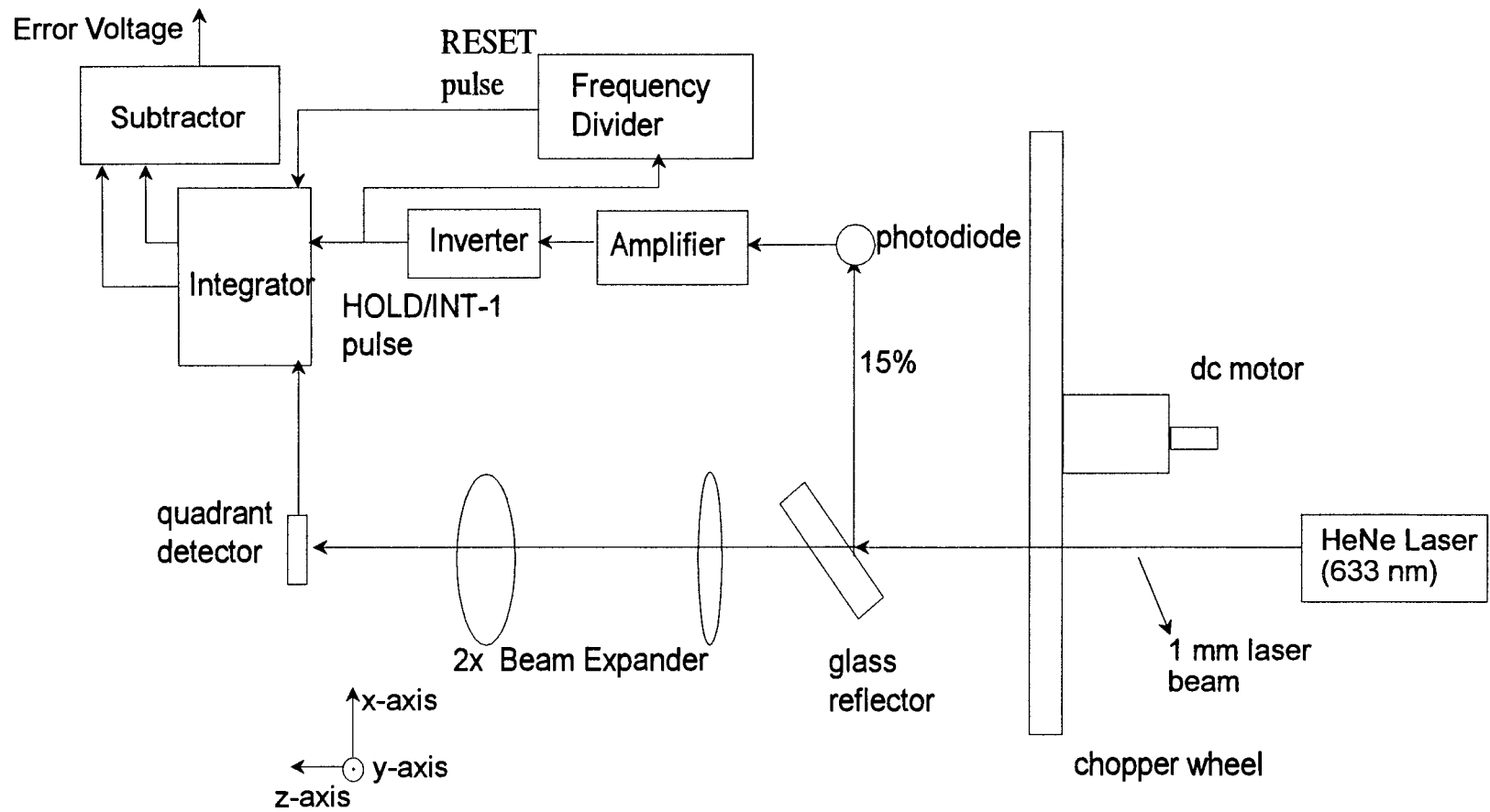


Figure 10 Test setup of the electrometer circuit

out in the form of a sector. When this chopper wheel was rotated at a speed of 1500 RPM, the output was a pulsed laser of frequency 25 Hz, whose pulse width was a function of the angle subtended by the narrow sector at the center of the wheel.

A fraction of the pulsed laser beam was diverted to a laser diode using a small glass flat as a reflector. The glass flat reflected about 15% of the incident light toward the photodiode. The current produced by this PIN silicon photodiode was used to generate the timing/control signals for the integrator AD2101.

If the detector was to respond to the slightest change in image position, the spot should be incident completely on the photosensitive area at all times. It may be recalled that the four quadrants in the detector are separated from each other and the 1.27 mm central hole by a gap of 0.13 mm. The minimum diameter of the image spot should hence be $[1.27 + (2 \times 0.13)]$ mm. The HeNe laser output, 1 mm in diameter was expanded to twice its diameter by using two positive lens of focal lengths 33 cm and 65 cm.

The output of the laser diode was amplified and used to trigger pulse width modifier 1. This one shot generator provides a 200 microsecond wide pulse that was used as the HOLD/INT⁻¹ signal for the AD2101 integrator. The circuit had to be reset after a few INT pulses. In this setup the RESET signal was generated as a fraction of the frequency of the HOLD/INT-1 pulses, by using a frequency divider. Two quadrant currents were simultaneously converted to voltages in this setup. These voltages were numerically subtracted, using the differential amplifier AD620 as a subtractor, to obtain the error voltage that represents the measure of beam drift.

The circuit was tested as follows. Error in alignment was created by small changes

in the position of the translation stage along the two axes in the transverse plane of the beam. The corresponding voltages from two quadrants were subtracted and plotted against the displacement. The graph in Figure 11 shows a relatively linear response of the circuit. The sensitivity of the circuit to beam alignment can be represented as the slope of the linear fit of the graph in Volts/mm. The sensitivity of the designed electrometer circuit to changes in beam position along the x-axis was 21 V/mm and along the y-axis 22.4 V/mm.

4.2.2 The Control Circuit

The movement in the beam position is corrected by realigning the optic fiber with reference to the beam. In the proposed circuit the translation stage that houses the fiber-detector is moved with the help of motors. The design was tested for motion along one of the axes normal to the optic axis. Instead of connecting the motor itself to the stage, the motor 'on' time along each direction, forward and reverse, was indicated by two separate LEDs. Figure 12 shows the test setup as a block diagram. The error voltage representative of beam alignment, is rectified using a diode bridge rectifier and compared continuously with the voltage on a capacitor. The charge on the capacitor is incremented by the current from a constant current source. The comparator 1 stays 'HIGH' long as the charge on the capacitor is less than the error voltage. Output of comparator 1 is used to bias transistor 1 which activates a relay coil. Either LED is selected depending on the way the relay is activated, which in turn is dependent on the polarity of the error voltage. Comparator and transistor 2 respond to the polarity of the error voltage and turns one of

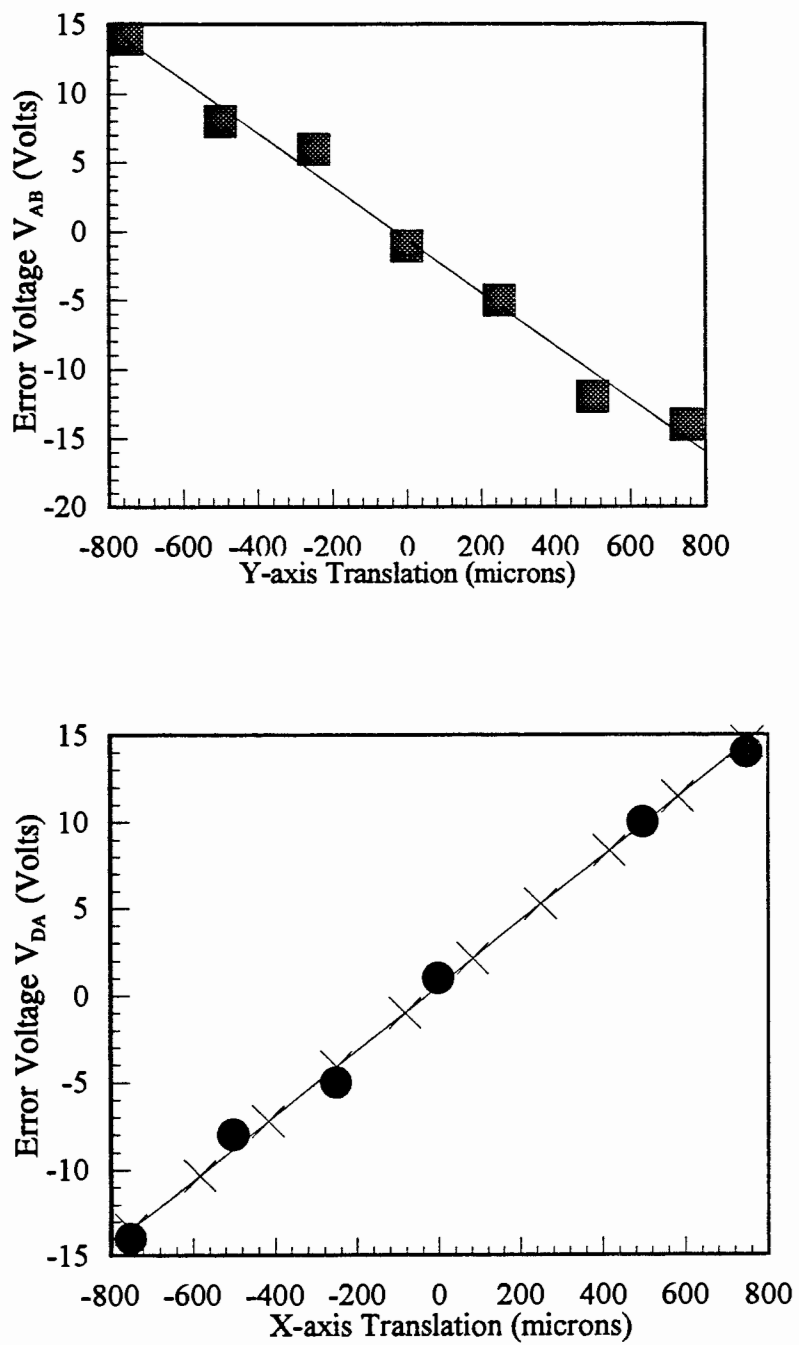


Figure 11. Response of the electrometer circuit

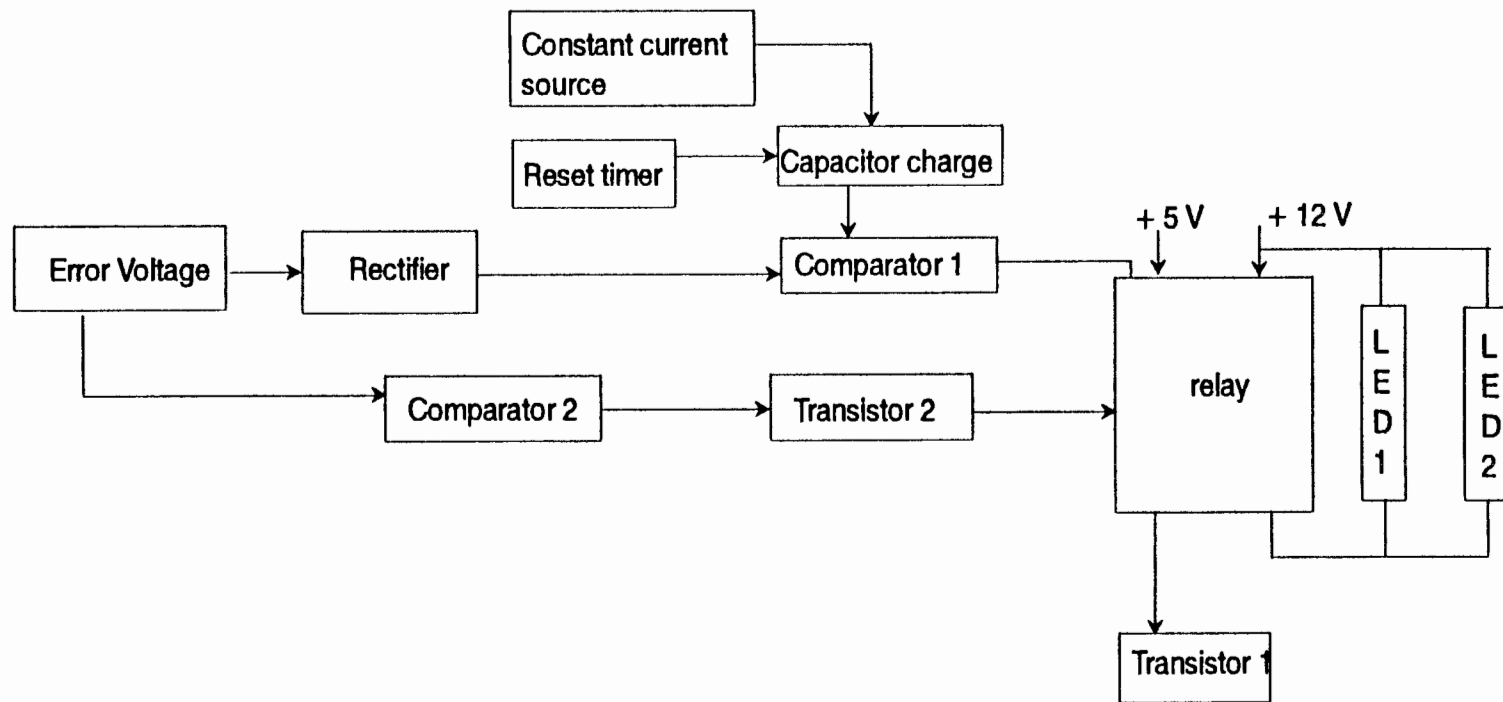


Figure 12. Test setup of the control circuit

the two LEDs 'on'. Table 2 indicates the sequence of logic in the control circuit for two sample values of the error voltage.

Table 1. Logic of the control circuit.

Error Voltage (V)	Comp 1	Transistor 1	Comp 2	Transistor 2	LED 1	LED 2
+ 3 V	HIGH	ON	HIGH	ON	OFF	ON
- 3 V	HIGH	ON	LOW	OFF	ON	OFF

Initially the position of the stage, where the beam was absolutely centered, was identified. While testing the circuit, the beam was misaligned by moving the translation stage from its null position to create an error voltage. When the error voltage was increased, the LEDs remained 'on' for a longer time. When the error was changed from positive to negative, the other LED was switched 'on' by the relay. The sensitivity of the circuit could not be numerically determined since the motors were not connected. It was noted that the error voltages -1 V to +1 V could not be accurately represented as the LED 'on' time. This was because an error voltage as small as 1 V, results in a motor 'on' time of a few milliseconds that cannot be resolved by the human eye in terms of the 'on' time of an LED. If however the motor was connected, a few millisecond duration would cause the motor to move the stage by a few hundred microns.

Chapter 5

Conclusion

An automatic system that can detect and correct for image spot drift on the optical fiber surface was designed. The circuits were tested at a breadboard level. The electrometer circuit measures and compares the currents from opposing quadrants of the detector to determine beam alignment with respect to the fiber surface, as an error voltage. The sensitivity of the circuit was 21 V per mm of beam motion along the x-axis, and 22.4 V per mm of movement along the y-axis. The control circuit operates on the error voltage and causes the DC motor to reposition the fiber-detector assembly with respect to the received image spot. The circuit was tested for motion along one axis. The motor 'on' time was visually read out as the 'on' time of an LED. Two LEDs represent the motor 'on' time in the forward and reverse direction. The design is yet to be tested with the motor installed in the LAMP system.

The design relies significantly on the efficiency of the quadrant detector. There exists a few inherent problems with this particular detector. The hole in the center of the detector, and the gap between quadrants, restricts its application to image spots that are greater than 1.53 mm in diameter. The gap also results in a small region of indecision. The currents produced by the quadrant detector when placed in the LAMP system were on the order of nanoamperes. If the circuit has to be adapted into the system, the signal must be amplified. Also the electrometer must integrate for a longer time in order to obtain a significant error voltage.

The following improvements on the current design are suggested as a possible effort to enhance the automatic beam alignment circuit. A quadrant detector with no hole in the center can make the circuit sensitive to smaller beam diameters. However the advantage in direct detection and correction of the problem is lost. The daytime capability of the LAMP system can be adopted into the automatic beam alignment circuit by using narrow band filters ahead of the quadrant detector.

References

- 1 Edited by E. D. Hinkley, "Laser Monitoring of the Atmosphere", published by Springer-Verlag, New York, 1976.
- 2 M. M. Sokoloski, "Laser Applications in Meteorology and Earth and Remote Sensing", SPIE Proceedings, 1062 (contains several articles by different authors) Jan 1989.
- 3 R. M. Measures, "Laser Remote Sensing -Fundamentals and Applications", New York, Chapters 9 and 10 (pg 320-460), 1992.
- 4 C. F. Bohren, D. R. Huffman, "Absorption and Scattering of Light by Small Particles", Wiley-Interscience, New York, 1983.
- 5 R. M. Measures, " Laser Remote Sensing-Fundamentals and Applications", New York, Chapters 2 and 3 (pg 11 -120), 1992.
- 6 D. W. Machuga, "Daytime Performance of the Lamp Rayleigh/Raman Lidar System", Penn State University, Masters Thesis in Electrical Engineering, May 1993.
- 7 T. D. Stevens, "An Optical Detection System for a Rayleigh/Raman Lidar", Penn State University, Masters Thesis in Electrical Engineering, August 1992.
- 8 P. A. Haris, "Performance Analysis of the LAMP Rayleigh/ Raman Lidar system", Penn State University, Masters Thesis in Electrical Engineering, December 1992.
- 9 Edited by S. C. Barden, "Fiber Optics in Astronomy", ASP Conference Series, 3, 1988.
- 10 M. Bartosewez, and J. Tyburski, "Wavefront Tilt and Beam Walk Correction for a Pulsed Laser System," SPIE proceedings 608, 24-28, 1986 .
- 11 P. J. VanArsdall, and R. J. Reeves, "Image processing for Automatic alignment in the Nova Laser Facility", SPIE proceedings, 608, 29-40, 1986.
- 12 M. C. Rushford, and P. J. Kuzmenko, "Pointing Alignment by Orthogonal phase-

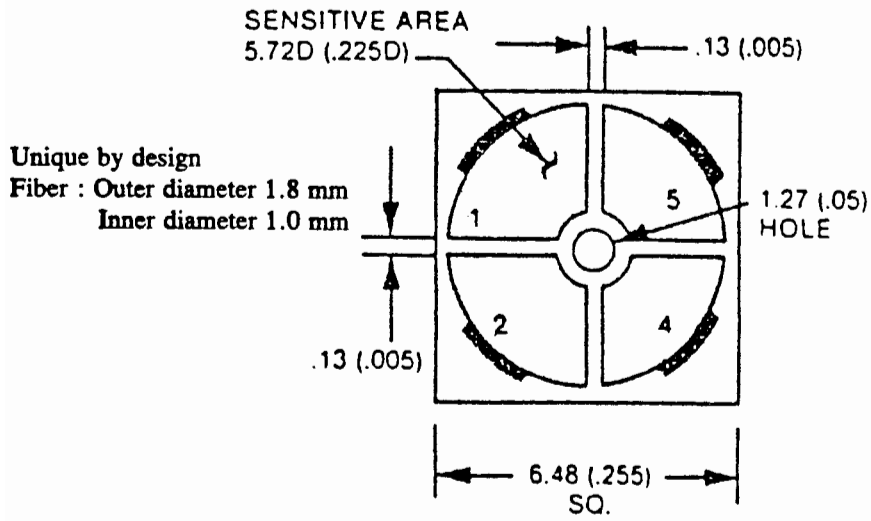
- lock feedback loops", SPIE proceedings, 608, 41-46, 1986.
- 13 C. R. Philbrick, D. B. Lysak, T. D. Stevens, P. A. T. Haris and Y.-C. Rau, "Lidar measurements of middle and lower atmosphere properties during the Ladimas campaign", Proceedings 11th ESA Symposium, 93.
 - 14 Tim D. Stevens, Paul A. T. Haris, Yi-Chung Rau and C. R. Philbrick, "Latitudinal Lidar mapping of stratospheric particle layers", Advanced Space Research, 14, No. 9, 193-198, 1994.
 - 15 P. A. T. Haris, T. D. Stevens, S. Maruvada and C. R. Philbrick, "Latitudinal variation of middle atmospheric density and temperature", Advanced Space Research, 14, No. 9, 83-87, 1994.
 - 16 C. R. Philbrick, D. B. Lysak, T. D. Stevens, P. A. T. Haris and Y.-C. Rau, "Atmospheric Measurements Using the LAMP Lidar during the LADIMAS Campaign", Sixteenth International Laser Radar Conference, NASA CP-3158,651-654, 1992.

Appendix A

The Quadrant Detector

The Quadrant Detector

43



Electrical properties of the Quadrant detector.

Detector Model Number	SD 225-23-21-040
Size (dia)	5.72 mm
Effective Area	4.1 mm ²
Gap	0.13 mm
Package Type	T0-8
Dark Current I_p @ $V_R = 10V$	2.8 nA
Temperature Dependence of Dark Current	1.09
Shunt Resistance R_{SH} @ $V_R = 10$ mV	10 M Ω (min) 500 M Ω (typ)
Junction Capacitance	100 pF (@ $V_R = 0V$) 25 pF (@ $V_R = 10V$)
Spectral Range	400-1100 nm
Radiant Sensitivity	0.35 A/W (He-Ne-633nm) 0.50 A/W (GaAs LED-930 nm) 0.20 A/W (YAG Laser-1060 nm)
Uniformity of Response	5%
Response time @ 655 nm	80 ns (@ $V_R = 0V$) 40 ns (@ $V_R = 10V$)
Maximum Reverse Voltage Breakdown	75 V
Maximum Light Power Density	10 mW/cm ²
Maximum Forward Voltage	0.7 V
Maximum Operating Temperature Range	-10 to +70°C
Maximum Storage Temperature Range	-25 to +100°C

Appendix B

The Electrometer Circuit

Appendix C

The Control Circuit

